Structural and thermoelectric properties of undoped IV-VI epitaxial films alloyed with tin

J. König, J. Nurnus, R. Glatthaar, H. Böttner, A. Lambrecht
Fraunhofer Institute for Physical Measurement Techniques (IPM)
Heidenhofstr. 8, 79110 Freiburg, Germany
email: joachim.nurnus@ipm.fhg.de

Abstract

IV-VI-compounds are well known materials with favourable thermoelectric properties at elevated temperatures (~700 K). Using related mixed crystals the thermoelectric properties can be optimised due to alloy scattering which leads to a decrease of the thermal conductivity without changing the other thermoelectric properties significantly. This method is well known as Joffe concept. The Joffe concept is about 50 years old and successfully proved several times using bulk crystals. But only few data exist about semiconductor thin films. Here we report on structural (SEM-, EDX-, XRD-, FT-IR-analysis) and in particular thermoelectric properties (Seebeck coefficient and Hall-Effect measurements for carrier concentration, conductivity and mobility) of molecular beam epitaxy (MBE) grown thin film based on the "Joffe-systems" (Pb,Sn)Se and (Pb,Sn)Te. Special care was taken to evaluate the in-plane thermal conductivity of insulated free standing (Pb,Sn)Se thin films.

With increasing tin concentrations increasing charge carrier concentration as well as increasing thermopower values were observed. The bandgap decreased with increasing tin concentration – shifting the optimum operating temperatures towards room temperature – and also the lattice thermal conductivity decreased as expected due to alloy scattering. All these effects strongly improve the thermoelectric properties of Sn-alloyed IV-VI epitaxial layers in the room temperature region.

Introduction

For applications in the region of 300 K normally V-VI compounds based on solid solutions of Bi_2Te_3, Bi_2Se_3 and Sb_2Te_3 are used. Up to now these compounds show the highest figures of merit (FOM) and therefore have the best efficiencies in thermoelectric devices designed for room temperature use. A striking disadvantage of these V-VI-compounds is the lamellar crystal structure leading to strong anisotropies of almost all physical properties relevant to thermoelectric (e.g. thermal and electric conductivity) and thin film growth (e.g. linear thermal expansion coefficient). These anisotropies complicate the use of V-VI compounds in thin film thermoelectric devices. Either the favourable properties of single crystalline films are found parallel or perpendicular to the substrate. Therefore – depending on the crystalline orientation of the substrates used to deposit epitaxial thin films – only applications exploiting in-plane (e.g. thermopiles) or cross-plane (e.g. Peltier coolers) will show optimum performance. In the case of a polycrystalline thin film the FOM will be determined by the distribution of the crystallographic orientations of the grains weighted with the respective thermoelectric properties in the direction of the respective driving force (temperature gradient for thermogenerators or electric current for Peltier coolers). Although high FOM-values for V-VI-superlattices [1] were reported up to now no devices exploiting these enhanced material properties are known. For the case of polycrystalline V-VI materials with an reduced average FOM miniaturized Peltier coolers [2] were successfully realized.

For IV-VI – based superlattices a high FOM has been reported by Harman [3], however no practical devices with this material are realised so far.

In contrast to the V-VI-compounds IV-VI-based compounds possess the cubic NaCl-crystal structure and almost isotropic physical properties. Therefore in this material system polycrystalline thin films could be as good as – or due to a reduced thermal conductivity because of grain boundary scattering even better than – polycrystalline V-VI thin films.

An epitaxial map (energy gap vs. lattice constant) of the lead salts compared to commonly used substrate materials for lead chalcogenide epitaxial growth and possible ternary components is shown in figure 1.

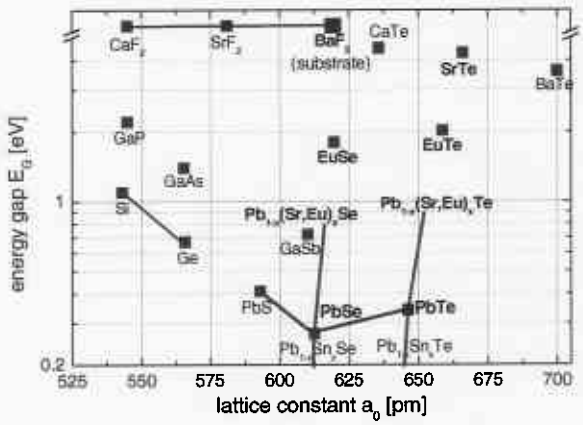

Fig. 1: Epitaxial map of the lead chalcogenides, possible ternary components and common substrate materials.

In the following the structural and thermoelectric properties of undoped epitaxial $Pb_{1-x}Sn_xSe$ and $Pb_{1-x}Sn_xTe$ thin films grown by MBE are be investigated.

IV-VI epitaxial thin film growth and characterisation

The investigated films were grown in an EPI 930 MBE system equipped with a PbSe and a PbTe compound source, a tellurium source and a selenium cracker cell necessary to compensate the Se- or Te-loss in the compound source. Prior to the growth 1 cm^2 BaF_2 substrates were freshly cleaved and fixed to the substrate holder using an InGa eutectic. In the load chamber the substrates were heated to 180 °C for 18 minutes to remove water from the substrate surface. An additional thermal cleaning step (425 °C for 25 minutes) was done in the growth chamber. Then the substrates were cooled down to growth temperature of 370 °C (thermocouple reading). The flux ratios of the PbSe (PbTe) and Se (Te) were chosen as 10:1 to guarantee a sufficient stabilization. The growth rate was about 1.4 µm per hour.

X-ray diffractometry-measurements were used for the determination of lattice constants and Θ/2Θ-scans are performed for phase analysis for the $Pb_{1-x}Sn_xSe$-layers (figure 2). In Figure 3 the decrease of the lattice constant a_0 with increasing tin content in PbSnSe is shown.

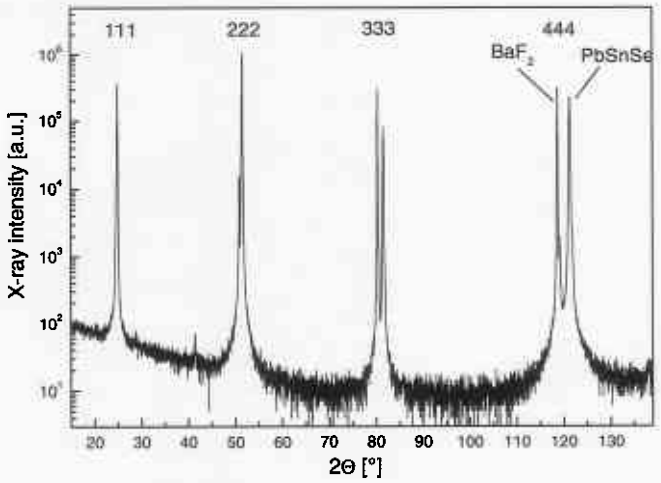

Fig. 2: X-ray diffraction Θ/2Θ-scan (Cu $K_{\alpha 1}$) of a $Pb_{0.94}Sn_{0.06}Se$-film on a (111) BaF_2 substrate measured at Fraunhofer-IAF.

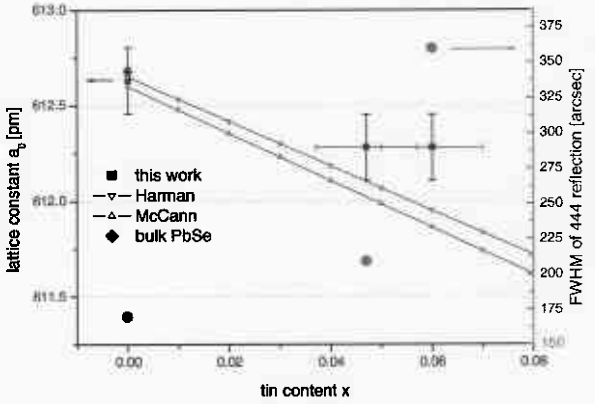

Fig. 3: Lattice constant a_0 and full width at half maximum (FWHM) of PbSnSe films on BaF_2 (111) at 300K determined by X-ray diffraction measurements versus Sn-content in comparison with literature data [15], [16].

After the growth the layers were investigated using Fourier transform infrared spectroscopy (FTIR) in order to determine the dependence of the absorption edge of the $Pb_{1-x}Sn_xSe$ and $Pb_{1-x}Sn_xTe$ layers on the tin concentration. Figure 4 shows measured infrared transmission spectra of the $Pb_{1-x}Sn_xSe$ layers and of an uncoated BaF_2 substrate. Besides the absorptions due to BaF_2 (~ 700 cm^{-1}) the interference fringes with an almost equidistant spacing $d\upsilon = n \cdot d/2$ (n = refractive index, d = film thickness) can be seen clearly. Knowing the refractive index of the thin film, the film thickness can thus be determined in principle from the FTIR spectrum. Since the refractive index of the films depends on the Sn concentration the film thickness were determined by secondary electron microscopy (SEM) as shown in figure 5. Besides the film thickness also surface morphology was determined by SEM analysis. The Sn-concentration was investigated using EDX up to ±0.5 at% accuracy. Using these Sn-contents the compositions of the samples were calculated.

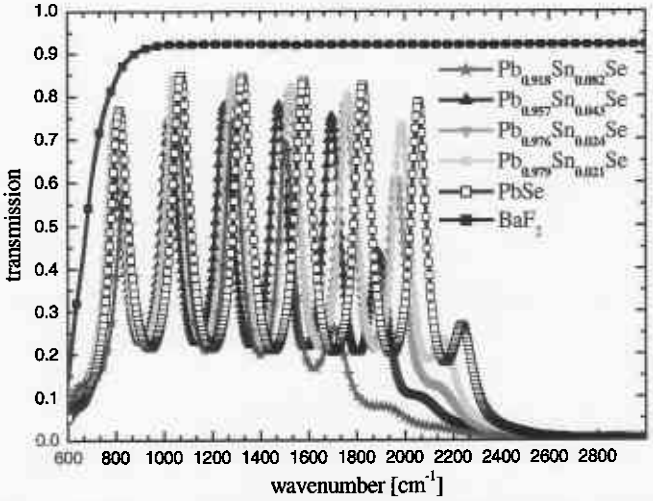

Fig. 4: FTIR transmission spectra of $Pb_{1-x}Sn_xSe$ samples with different Sn concentrations and of an uncoated BaF_2 substrate.

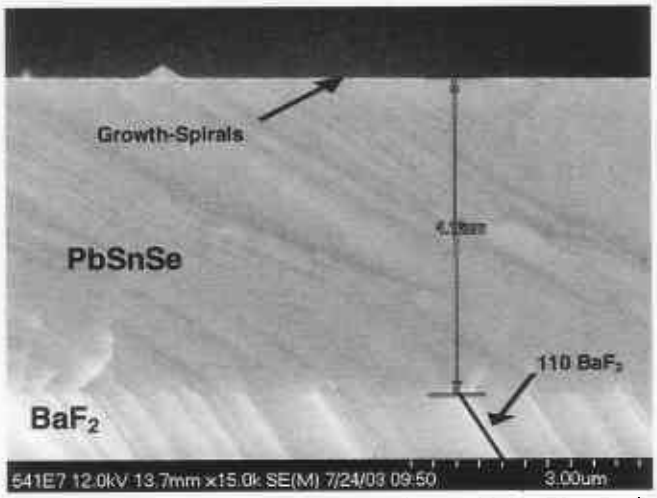

Fig. 5: SEM measurement of a 4.16 µm thick $Pb_{1-x}Sn_xSe$ sample grown on a (111) BaF_2 substrate.

The thermopowers of the samples were measured at room temperature. During the measurement a temperature gradient of 10 K was applied to generate the Seebeck voltage. The results are shown in figure 6. It is obvious, that the measured thermopower values decrease with increasing Sn-content.

The electrical conductivities and charge carrier concentrations were determined by temperature dependent Hall measurements using the van-der-Pauw method. The samples were thermally contacted to a cooled copper heat sink using silver glue, the electrical contacts were realized by gold wires soldered onto the corners of the samples using In-solder. During the measurement electrical currents in the region of ±5 mA and magnetic fields of 0.2 Tesla were used. The measured mobilities and charge carrier concentrations in the temperature range from 40 K to 320 K are shown in figure 7a and b. With increasing Sn content the mobility at room temperature increases whereas the mobility rise towards lower temperatures decreases with increasing Sn content.

The measured charge carrier concentrations are almost temperature independent, with increasing Sn-content the concentration rises up to $4 \cdot 10^{18}$ cm^{-3} for PbSnSe (x = 0.08) and for PbSnTe (x = 0.12) up to $6 \cdot 10^{18}$ cm^{-3}.

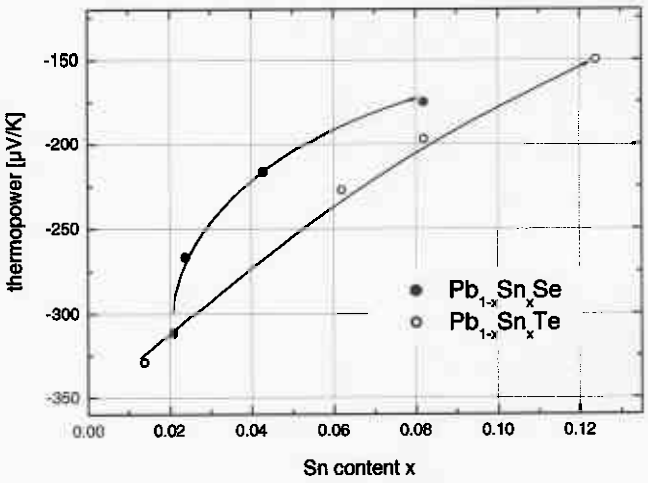

Fig. 6: Room temperature thermopower values of the investigated $Pb_{1-x}Sn_xSe$ and $Pb_{1-x}Sn_xTe$ samples.

In order to complete the thermoelectric properties, in-plane thermal conductivity measurements using a bridge method were performed on the PbSnSe samples. Details on the thermal conductivity measurements are given elsewhere [4], [5].

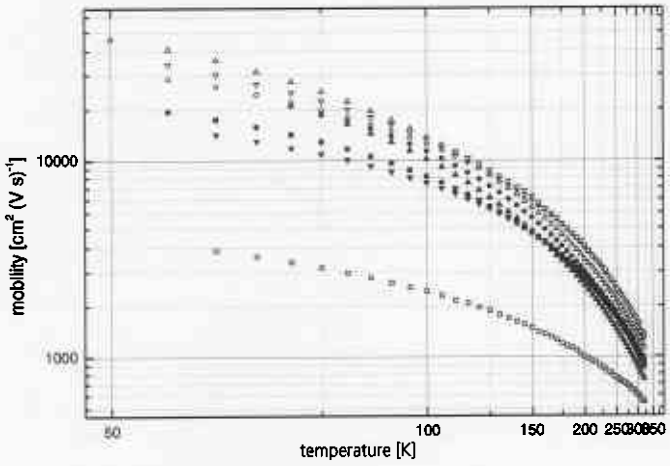

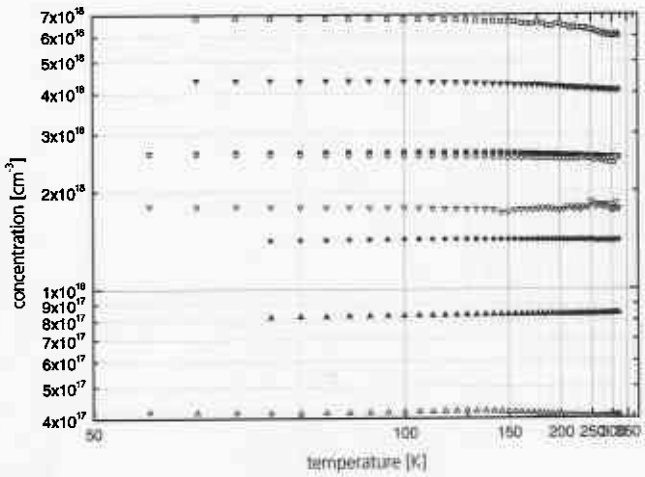

Fig. 7: Temperature dependent mobilities (a) and charge carrier concentrations (b) ■ $Pb_{0.957}Sn_{0.043}Se$; ● $Pb_{0.976}Sn_{0.024}Se$; ▲ $Pb_{0.979}Sn_{0.021}Se$; ▼ $Pb_{0.918}Sn_{0.082}Se$; □ $Pb_{0.876}Sn_{0.124}Te$; ○ $Pb_{0.918}Sn_{0.082}Te$; △ $Pb_{0.986}Sn_{0.014}Te$; ▽ $Pb_{0.938}Sn_{0.062}Te$

For the evaluation of the measurements an emissivity of the samples of $\varepsilon = 0.3$ – independent of the Sn content of the samples – was assumed. The resulting in-plane thermal conductivity values are shown in figure 8. Within the experimental error the total thermal conductivity λ decreases with increasing Sn content of the films.

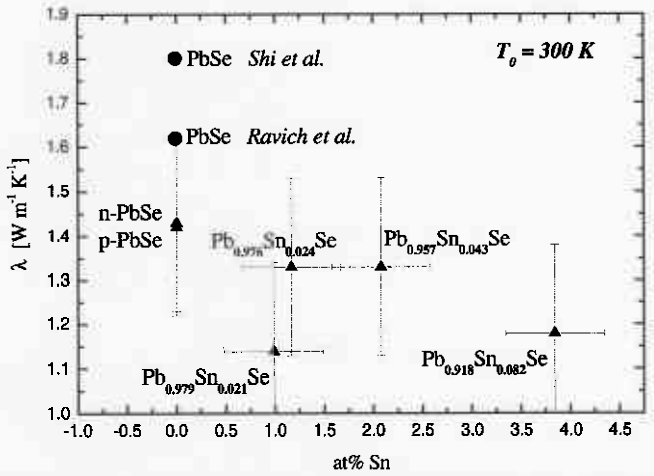

Fig. 8: Measured in-plane thermal conductivities of the investigated $Pb_{1-x}Sn_xSe$ samples. [7], [8]

Results and discussion

The absorption edge of the investigated IV-VI-samples decreases with increasing Sn-content (Fig. 9). Although the determined absorption edges are not corrected for the Moss-Burstein-Shift [6] – which would qualitatively result in slightly lower energies at higher charge carrier concentrations - a good agreement with literature data [9] – [13] can be found.

It is well known, that materials with a band gap of $E_g \sim 4 \cdot k_B \cdot T$ (k_B: Boltzmann constant) are well suited for applications at a temperature T (e.g. Bi_2Te_3: $E_g \sim 150$ meV $\sim 6 \cdot k_B \cdot 300$ K).

Therefore the decreased bandgap in the investigated Sn-rich samples should result in an enhanced room temperature thermoelectric efficiency. It is known, that for binary PbTe and PbSe epitaxial films the optimum charge carrier concentrations for high FOMs are in the region from $8 \cdot 10^{18}$ cm^{-3} to $1 \cdot 10^{19}$ cm^{-3}. Since on the one hand side increasing Sn-contents result in increasing charge carrier concentrations and on the other hand increasing Sn-contents result in decreased band gaps, Sn has a double function in undoped lead chalcogenide films: It reduces the band gap and at the same time acts as a dopand. According to phase diagrams that can be found in the literature [14], [15] valid for crystals grown under equilibrium conditions p-type doping is found for Se (Te)-stabilized $Pb_{1-x}Sn_xSe$ ($Pb_{1-x}Sn_xTe$). The non-equilibrium MBE grown samples show n-type doping for Se-stabilized thin epitaxial films. The same effect was found for undoped, Te-stabilized $Pb_{1-x}Sn_xTe$ epitaxial films and confirmed by thermopower and Hall-measurements. Therefore the emplacement of Sn in our IV-VI compound thin films grown under non-equilibrium conditions significantly differ from those single crystals.

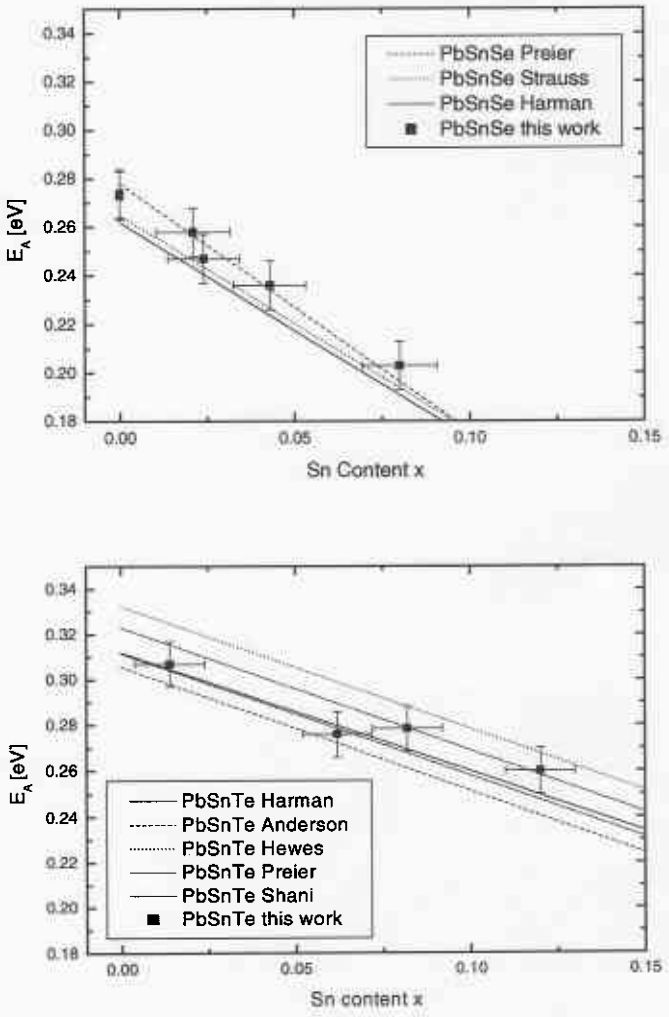

Fig. 9: Energy of the absorption edge of $Pb_{1-x}Sn_xSe$ and $Pb_{1-x}Sn_xTe$ samples respectively in comparison with literature data [9] – [13]

Using the experimentally determined charge carrier concentrations the electronic contribution λ_e of the thermal conductivity was determined under the assumption of parabolic energy bands. The effective masses m* used to calculate the reduced Fermi energies and Lorentz-numbers L were taken from [14]. The lattice thermal conductivities calculated by $\lambda_l = \lambda - \lambda_e$ for the $Pb_{1-x}Sn_xSe$ thin films are shown in figure 10. The effect of reduced λ_l values due to alloy scattering is obvious. For the sample with the highest Sn content $Pb_{0.92}Sn_{0.08}Se$ a lattice thermal conductivity of ~ 1 Wm^{-1}K^{-1} is found. Compared to the binary PbSe compounds with $\lambda_l \sim 1.4$ Wm^{-1}K^{-1} this corresponds to a reduction of λ_l by approximately 30 percent.

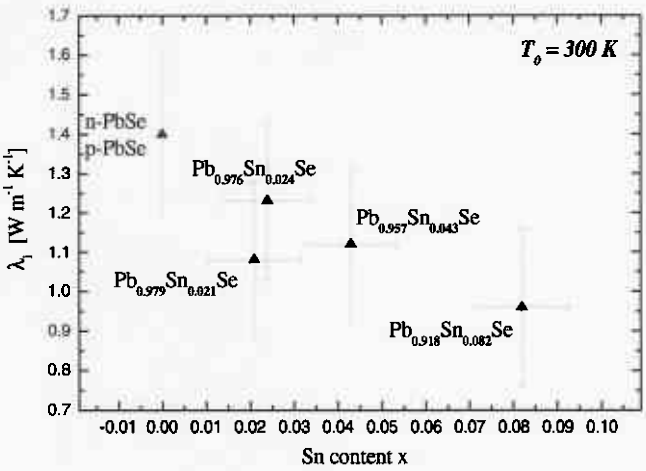

Fig. 10: Lattice thermal conductivities calculated from the measured total thermal conductivities by $\lambda_l = \lambda - \lambda_e$.

The room temperature properties of the investigated "undoped" IV-VI epitaxial films alloyed with tin are summarized in table 1 and compared with other for high FOM optimised IV-VI thin films. Binary PbSe films with carrier concentrations optimised for room temperature (~ $1 \cdot 10^{19}$ cm^{-3}) have FOM < 0.3. With increasing Sn content the FOM of the samples increases strongly even in these "undoped" samples. For $Pb_{0.918}Sn_{0.082}Se$ a very high value of ZT = 0.6 was determined.

A number of details are very promising that even higher FOMs can be realized within those unintentionally doped $Pb_{1-x}Sn_xSe$ epitaxial films: Optimised FOMs are expected for carrier concentrations in the region of $1 \cdot 10^{19}$ cm^{-3}. The experimental data presented indicate that these concentrations could be reached for $Pb_{0.825}Sn_{0.175}Se$ (s. table 1). For this compound a band gap of ~ 100 meV ~ $4 \cdot k_B \cdot T$ – that means almost ideal for room temperature applications – is expected. The extrapolated Seebeck coefficient for this concentration is ~ 135 µV/K. Finally due to the almost constant mobilities conductivities of 1400 Ω^{-1}cm^{-1} may be anticipated. Even though the lattice thermal conductivity is not reduced as much as for low Sn contents in this region ZT values of 0.8 at 300 K are expected from the extrapolated data within the system of unintentionally doped epitaxial $Pb_{1-x}Sn_xSe$ thin films.

Similar results are expected for $Pb_{1-x}Sn_xTe$. The powerfactor for $Pb_{1-x}Sn_xTe$ is higher than that for $Pb_{1-x}Sn_xSe$ with a comparable tin content, but the thermal conductivity is expected to be higher too. Thermal conductivity measurements of the $Pb_{1-x}Sn_xTe$ films are in progress.

Further improvements of the FOM are expected with PbSnSe/PbSnSeTe- or PbSnTe/PbSnSeTe-superlattices, similar to the results with PbSeTe-PbTe – SL[19] and PbTeSe-PbTe Quantum-Dot-SL [3].

Summary and outlook

It has been shown, that epitaxial $Pb_{1-x}Sn_xSe$ and $Pb_{1-x}Sn_xTe$ quasibinary films can reach thermoelectric figures of merit as high as 0.6 at room temperature. Main reason for this is the multifunctional effect of Sn in the thin film: Sn reduces the band gap towards values ideal for room temperature applications, Sn acts at the same time as a dopand increasing the charge carrier concentration towards 10^{19} cm^{-3} and last but not least reduces the thermal conductivity due to alloy scattering. The emplacement mechanisms for Sn in IV-VI-based compound non equilibrium MBE samples is not known up to now.

Extrapolating the presented results shows, that ZT = 0.8 could be reached within this system for $Pb_{0.825}Sn_{0.175}Se$ thin films. This value is still smaller than those known from standard Bi_2Te_3-based V-VI-compounds, nevertheless the expected isotropy of the $Pb_{1-x}Sn_xSe$ compounds could be a striking advantage. Due to isotropy such high – or due to enhanced phonon scattering at grain boundaries – even higher FOMs should be found in polycrystalline materials. Therefore the complicated deposition of single crystalline compounds for the use in high efficient thin film thermoelectric devices could be overcome by the material system presented in this paper.

n-type Material	**x** EDX	**λ** [W m^{-1} K^{-1}]	**Power** [µW/cm K^2]	**ZT**
PbSnSe	0.021	1.14	10.57	0.28
PbSnSe	0.024	1.33	16.35	0.37
PbSnSe	0.043	1.33	20.09	0.45
PbSnSe	0.082	1.18	23.69	0.6
PbSnTe	0.014		9.87	
PbSnTe	0.062		23.57	
PbSnTe	0.082		25.54	
PbSnTe	0.124		26.59	
PbSe * [17]		2.87	21.0	0.22
PbTe * [18]		4.15	31.6	0.23
$PbSe_{0.2}Te_{0.8}$-PbTe -SL [19]		1.87	28.0	0.45

Table 1: Experimental data of $Pb_{1-x}Sn_xSe$ and $Pb_{1-x}Sn_xSe$ samples in comparison with literature data.
* optimised carrier concentration

Acknowledgements

This work was partly supported by BMBF grant no. 03N1084.

The XRD-measurements were performed by Dr. L. Kirste at Fraunhofer IAF.

References

1. Venkatasubramanian, R. et al., "Thin-film thermoelectric devices with high room-temperature figures of merit", Nature, Vol. 413 (2001), pp. 597-602.
2. Böttner, H. et al., "New Thermoelectric Components Using Microsystem Technologies", IEEE Journal of Microelectromechanical Systems, Vol. 13, June 2004, pp. 414.
3. Harman, T. C., et al., "Quantum Dot Superlattice Thermoelectric Materials and Devices", Science 2002 Vol. 297, pp. 2229-2232.
4. Völklein, F. et al., "Methods for thermal conductivity measurement and thermal diffusity of very thin films and foils", Measurement, Vol. 5, 1987, p. 38,.
5. Nurnus, J., et al., "Structural and Thermoelectric Properties of Bi_2Te_3 Based Layered Structures", Proc. 19th Int. Conf. Thermoelectrics, Cardiff (U.K.) 21. – 25. August 2000, p. 236.
6. Pankove, "Optical Processes in Semiconductors", Dover Publications, New York, 1975.
7. Ravich, Efimova, Smirnov: "Semiconducting Lead chalcogenides"; Plenum Press; 1970.
8. Shi, Z., et al., "IV-VI compound midinfrared high-reflectivity mirrors surface-emitting lasers grown by molecular-beam epitaxy", Appl. Phys. Lett. Vol. 76, 2000, p. 3688.
9. Preier, H., "Recent advances in Lead-Chalcogenide diode lasers", Appl. Phys., Vol. 20, 1979, p. 189.
10. Strauss, A. J., "Inversion of conduction and valence bands in $Pb_{1-x}Sn_xSe$ alloys", Phys. Rev., Vol. 157, 1967, p. 608.
11. Hewes, C. R.; "Nuclear-Magnetic-Resonance studies in PbTe and $Pb_{1-x}Sn_xTe$. An experimental determination of k · p band parameters and magnetic hyperfine constants", Phys. Rev. B 7; 1973; p.5195.
12. Anderson, W. W., " Gain-frequency-current relation for $Pb_{1-x}Sn_xTe$ double heterostructure lasers", IEEE J. Quantum Electron. QE-13; p.532
13. Shani, Y., "Calculation of the refractive indexes of lead chalcogenide salts and its application for injection lasers", IEEE J. Quantum Electron. QE-13; p.51
14. Landolt-Börnstein: Vol. 17d: "Semiconductor", Springer-Verlag, Heidelberg, 1984.
15. Harman, T. C., et al., "Narrow Gap Semiconductors", Applied Solid State Science, Vol. 4, 1974, p.1.
16. McCann, P. J., "Liquid phase epitaxy growth of PbSnSeTe alloys lattice matched with BaF_2"J. Appl. Phys. Lett. Vol 75, 1994, p. 1145.
17. Beyer, H., dissertation University Linz, 2000.
18. Beyer, H.,"Highly Efficient IV-VI MQW and Superlattice Structures", Proceedings 19th International Conference on Thermoelectrics, 2000, p.28-36
19. Lambrecht, A., "High Figure of Merit ZT in PbTe and Bi_2Te_3 Based Superlattice Structures by Thermal Conductivity Reduction", Proc. 20th International Conference on Thermoelectrics, ISBN 0-7803-7205-0, 2001, p. 335-9.